The role of Turbulent Convection and wind in Geostrophic Circulation: Direct Numerical Simulation Study

Smruti Ranjan Jena[1,3], Bishakhdatta Gayen[1,3], Catherine A. Vreugdenhil[2] and Ross Griffiths[1]

[1]Research School of Earth Sciences
Australian National University, Canberra, ACT 0200, Australia

[2]Department of Applied Mathematics and Theoretical Physics
University of Cambridge, Cambridge CB3 0WA, UK

[3]ARC Centre of Excellence for Climate Extremes
Australian National University, Canberra, ACT 0200, Australia

Abstract

Direct numerical simulations (DNS) are used over a three-dimensional rotating basin under geostrophic rotation, in order to understand the relative roles of buoyancy and wind stress on the heat and mass transport. Our main focus is on the large Rayleigh number regime (*Ra*, being the measure of buoyancy forcing) which is the order of 10^{12} to sustain turbulent convection. We also maintained small values of convective Rossby number $Ro \sim 0.1$ at a fixed Prandtl number, $Pr \sim 5$ while imposing a meridional wind stress pattern.

Introduction

The classical belief delineates the fact that ocean is predominantly driven by mechanical forces as it provides major energy input to maintain stratification. In this regard, Munk & Wunsch [9] emphasized that wind & tides are the only possible factors that provide mechanical energy input to the oceans. Kuhlbrodt et al. [6] also supported the fact from a computational & observational standpoint that wind causes the turbulent mixing which drives the Atlantic Overturing Circulation (AMOC). While examining the mechanical energy budget of ocean, Wang & Huang [15] stated that energy input from wind & tidal dissipation, geothermal heating is much larger than the input from the thermal forcing. The role of surface thermal forcing (heating and cooling over the upper boundary) is unclear from these established results.

On the other hand, horizontal variation of surface buoyancy, known as horizontal convection, can drive the large-scale overturning in the ocean [1, 2, 8, 10, 11]. Hughes & Griffiths [4, 5] illustrated the feasibility of ocean overturing being a convective process. Some of the recent works [3, 7] also showed the significance of buoyancy in the deep overturning of the Southern Ocean in model simulation considering both wind & buoyancy. Scotti & White [12] showed that the circulation driven by surface buoyancy forcing is very efficient in producing mixing. Gayen et al. [1, 2] confirmed numerically that buoyancy forcing leading to horizontal convection can be a potential co-driver in the overturning circulation. Moreover, recent study on the model Southern Ocean [13] has estimated that turbulent mixing in this region has enhanced by buoyancy driven processes like convection and baroclinic eddies.

Recent works on rotating horizontal convection in an idealized closed basin using direct simulations by Vreugdenhil et al. [14] showed that maximum percentage of energy supplied through the buoyancy flux completely goes into the irreversible mixing. Same study showed that surface buoyancy

forcing could form intensified boundary currents in the presence of side boundaries, which further control heat and mass transport. However, effect of mechanical forcing in the presence of turbulent convection for the closed basin flow that is dynamically similar to North-Atlantic has not been studied before. Building upon the insight obtained in the previous attempts [2,14], we aim to examine the role of mechanical and buoyancy forcing on the flow and heat/mass transport under planetary rotation in an idealized closed basin.
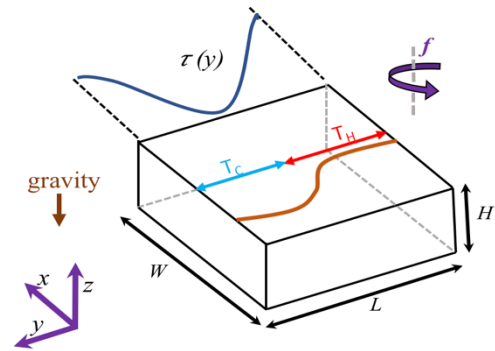

Figure 1. Schematic of the flow domain, with half of the top surface heated & half of it is cooled. Wind stress τ(y) is applied over top boundary using vertical gradient of the zonal velocity u.

Governing parameters & Model Setup

An idealized three-dimensional box of length L, width W and height H is chosen for simulating the flow in a closed domain, dynamically similar to a North Atlantic Basin (as shown in figure 1). The non-dimensional parameters that govern the flow are, Rayleigh number, Rossby number, Prandtl Number Ekman number and the aspect ratios are represented as, respectively,

$$Ra = \frac{g\beta\Delta T L^3}{\nu\kappa} \ , Ro = \frac{U}{Lf}, \ Pr = \frac{\nu}{\kappa} \ , E = \frac{\nu}{L^2 f} \ , B = \frac{W}{L} \ , D = \frac{H}{L},$$

where g = acceleration due to gravity, α = coefficient of thermal expansion, f = Coriolis parameter, U refers to the velocity scale $\sim \sqrt{g\beta\Delta T H}$, $\Delta T = T_H - T_C$ i.e. the imposed thermal forcing, ν and κ are the molecular viscosity and molecular diffusivity, respectively. In addition, we introduced a new parameter to characterize the influence of wind [13] as

$$S = \frac{\tau_{max}}{\rho_0 g\beta\Delta T H},$$

where, τ_{max} = maximum wind stress, ρ_0 = reference density. The governing equations for solving the flow, we solve continuity, momentum and heat equation in their non-dimensional form as follows:

$$\nabla \cdot \hat{u} = 0 \qquad (1)$$

$$Pr^{-1}\left(\frac{D\hat{\boldsymbol{u}}}{D\hat{t}} + \nabla\hat{p}\right) = \nabla^2\hat{\boldsymbol{u}} - Ra\hat{T}\hat{k} - E^{-1}\hat{\boldsymbol{k}} \times \hat{\boldsymbol{u}} \qquad (2)$$

$$\frac{D\hat{T}}{D\hat{t}} = \nabla^2\hat{T} \qquad (3)$$

Direct Numerical Simulation (DNS) is used [14] to solve an incompressible, non-hydrostatic Navier-Stokes equation with a non-inertial frame of reference considering the Boussinesq approximation with a linear equation of state. Rotation is introduced taking β-plane approximation into consideration. In the present simulation, a *tan-hyperbolic* temperature profile is implemented on the top boundary to provide a temperature distribution i.e. half way cooled & halfway heated to a uniform temperature of T_C & T_H, respectively (ref. figure 1). A meridional wind stress pattern is imposed at the top surface in terms of the vertical velocity gradient. Adiabatic wall condition is used in junction with no-slip boundary for velocity, both on the side walls and also on the bottom topography. The grid chosen for solving the present case is 768×256×256 with the more clustering near the wall so as to incorporate the effect of Ekman layer & Stewartson boundary layer. Table 1 showcases the various parameters for all the cases studied.

	Ra	*Ro*	*S*	*E*
Case-1	7.4×10^{11}	0.0861	0	5×10^{-7}
Case-2	7.4×10^{11}	0.0861	6.7×10^{-5}	5×10^{-7}
Case-3	7.4×10^{11}	0.0861	28.8×10^{-5}	5×10^{-7}
Case-4	7.4×10^{11}	0.0861	58.9×10^{-5}	5×10^{-7}

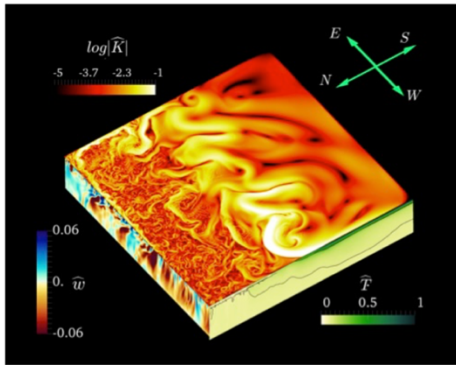Table 1. Tabulated data for different simulation cases.

Results & Discussion

Figure 2. Instantaneous contours of *Turbulent Kinetic Energy* ($\hat{k}$), *z-component of the velocity* ($\hat{w}$) and *temperature* ($\hat{T}$) for Case 2 ($Ra = 7.4 \times 10^{11}$ and $S = 6.7 \times 10^{-5}$) on the top plane, the northward plane and the westward plane respectively. Solutions are taken at a single time instant during the thermally equilibrated state.

We allowed the simulations to reach thermally equilibrated state when total heat flux from the top boundary is zero. The flow statistics are calculated over the thermally equilibrated state. Figure 2 illustrates a three-dimensional depiction of various flow variables, namely turbulent kinetic energy ($\hat{k}$), temperature ($\hat{T}$) and z-component of velocity ($\hat{w}$) in their non-dimensional form on the top plane, westward plane and northward plane, respectively. The varying coloured contours

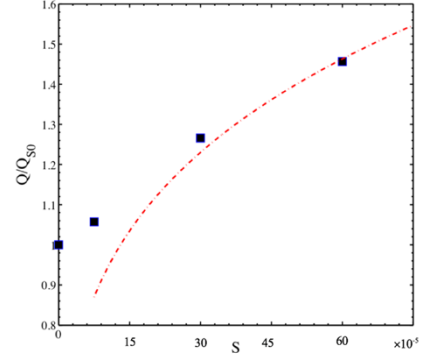on the northward plane confirms the presence of deep convective vortices, termed as "Chimneys" [14].

Figure 3. Variation of non-dimensional heat flux (Q/Q_{SO}) with Wind parameter (*S*). Line shows the 1/4th power of the wind parameter

Isotherms along the westward plane suggests a stable boundary layer over the stably heated zone and attains more instability over the cold part following enhanced convection near the northern half. Turbulent kinetic energy isocontours reveal a lot of information about the flow features that include intensification of surface current along western boundary, formation of eastward propagating geostrophic current. These contours suggest the dissipation in turbulent kinetic energy as the current moves across the domain and reached the northern boundary. It is observed that eddies are formed along the northern boundary and further shredded into the domain following a change in their scale.

We also estimated net heat uptake from the surface boundary for different wind stresses at a fixed Ra as shown in figure 2. The results suggest that heat uptake increases with increasing wind stresses due to increment of Ekman transport with larger wind forcing. The heat flux approximately varies as the 1/4th power of wind stress, in wind dominated region.

Conclusions

We studied effect of mechanical forcing on the flow, in the presence of turbulent convection, in a closed basin using DNS. Present simulations are able to capture vast scales of motions: from turbulent mixing of energy, through vertical convection to currents and large-scale gyre recirculation across basin. Basin scale overturning circulation is largely dominated by buoyancy forcing. Solutions show the formation of intensified surface current along with deep convective vortices. Wind, which plays a significant role in the net heat uptake to the system, increases heat transport with increase in wind forcing. Based on the observations, it can be concluded that present DNS resolves all the scales of motion and the insights obtained from the results can be used for modelling North Atlantic Ocean Circulation.

Acknowledgments

References

[1] Gayen, B., R. W. Griffiths, G. O. Hughes, and J. A. Saenz (2013), Energetics of horizontal convection, J. Fluid Mech., 716, R10.

[2] Gayen, B., Griffiths, R. W., and Hughes, G. O. (2014), Stability transitions and turbulence in horizontal convection, J. Fluid Mech., 751, 698–724.

[3] Hogg, A. M. (2010), An Antarctic Circumpolar Current driven by surface buoyancy forcing, Geophys. Res. Lett., 37, L23601.

[4] Hughes, G. O., and Griffiths, R. W. (2008), Horizontal convection, Annu. Rev. Fluid Mech., 40(1), 185–208.

[5] Hughes, G., and Griffiths, R. (2006), A simple convective model of the global overturning circulation, including effects of entrainment into sinking regions, Ocean Modell., 12(1–2), 46–79.

[6] Kuhlbrodt, T., Griesel, A., Montoya, M., Levermann, A., Hofmann, M., and Rahmstorf, S. (2007), On the driving processes of the Atlantic meridional overturning circulation, Rev. Geophys., 45, RG2001.

[7] Morrison, A. K., Hogg, A. M., and Ward, M. L. (2011), Sensitivity of the Southern Ocean overturning circulation to surface buoyancy forcing, Geophys. Res. Lett., 38, L14602.

[8] Mullarney, J. C., Griffiths, R. W. and Hughes, G. O. (2004), Convection driven by differential heating at a horizontal boundary, J. Fluid Mech., 516, 181–209.

[9] Munk, W., and Wunsch, C. (1998), Abyssal recipes II: Energetics of tidal and wind mixing, Deep Sea Res., Part I, 45(12), 1977–2010.

[10] Park, Y. G., and Whitehead, J. A. (1999), Rotating Convection Driven by Differential Bottom Heating, J. Phys. Ocean., 29, 1208–1220.

[11] Rossby, H. T. (1965), On thermal convection driven by non- uniform heating from below: an experimental study, Deep Sea Res., 12, 9–16.

[12] Scotti, A., and White, B. (2011), Is horizontal convection really "non-turbulent"?, Geophys. Res. Lett., 38, L21609.

[13] Sohail, T., Gayen, B., and Hogg, A. M. (2018), Convection enhances mixing in the Southern Ocean, Geophysical Research Letters, 45, 4198–4207.

[14] Vreugdenhil, C. A., Gayen, B., and Griffiths, R. W. (2016), Mixing and dissipation in a geostrophic buoyancy-driven circulation, Journal of Geophysical Research: Oceans, 121, 6076–6091.

[15] Wang, W., and Huang, R. X. (2005), An experimental study on thermal circulation driven by horizontal differential heating, J. Fluid Mech., 540, 49–73.